



This is a repository copy of *Mechanistic insights of 2,4-D sorption onto biochar: Influence of feedstock materials and biochar properties.*

White Rose Research Online URL for this paper:  
<http://eprints.whiterose.ac.uk/131067/>

Version: Accepted Version

---

**Article:**

Mandal, S., Sarkar, B. [orcid.org/0000-0002-4196-1225](https://orcid.org/0000-0002-4196-1225), Igalavithana, A.D. et al. (4 more authors) (2017) Mechanistic insights of 2,4-D sorption onto biochar: Influence of feedstock materials and biochar properties. *Bioresource Technology*, 246. pp. 160-167. ISSN 0960-8524

<https://doi.org/10.1016/j.biortech.2017.07.073>

---

**Reuse**

This article is distributed under the terms of the Creative Commons Attribution-NonCommercial-NoDerivs (CC BY-NC-ND) licence. This licence only allows you to download this work and share it with others as long as you credit the authors, but you can't change the article in any way or use it commercially. More information and the full terms of the licence here: <https://creativecommons.org/licenses/>

**Takedown**

If you consider content in White Rose Research Online to be in breach of UK law, please notify us by emailing [eprints@whiterose.ac.uk](mailto:eprints@whiterose.ac.uk) including the URL of the record and the reason for the withdrawal request.



[eprints@whiterose.ac.uk](mailto:eprints@whiterose.ac.uk)  
<https://eprints.whiterose.ac.uk/>

1 **Mechanistic insights of 2,4-D sorption onto biochar: Influence of feedstock materials**  
2 **and biochar properties**

3

4 Sanchita Mandal<sup>1</sup>, Binoy Sarkar<sup>1,2</sup>, Avanthi Deshani Igalavithana<sup>3</sup>, Yong Sik Ok<sup>3,6</sup>, Xiao  
5 Yang<sup>3</sup>, Enzo Lombi<sup>1</sup>, and Nanthi Bolan<sup>4,5\*</sup>

6

7 <sup>1</sup>Future Industries Institute (FII), University of South Australia, Mawson Lakes, SA 5095,  
8 Australia,

9 <sup>2</sup>Department of Animal and Plant Sciences, The University of Sheffield, Sheffield, S10 2 TN,  
10 UK

11 <sup>3</sup>Korea Biochar Research Center, Kangwon National University, Chuncheon 24341, Korea

12 <sup>4</sup>Cooperative Research Centre for Contaminant Assessment and Remediation of the  
13 Environment (CRC CARE), Mawson Lakes, SA 5095, Australia

14 <sup>5</sup>Global Center for Environmental Remediation, University of Newcastle, Callaghan, NSW  
15 2308, Australia

16 <sup>6</sup>O-Jeong Eco-Resilience Institute (OJERI) & Division of Environmental Science and  
17 Ecological Engineering, Korea University, Seoul, Korea

18

19 \*Corresponding author

20 Prof Nanthi Bolan

21 University of Newcastle

22 Email: [Nanthi.Bolan@newcastle.edu.au](mailto:Nanthi.Bolan@newcastle.edu.au)

23 Tel: +61 2 49138750

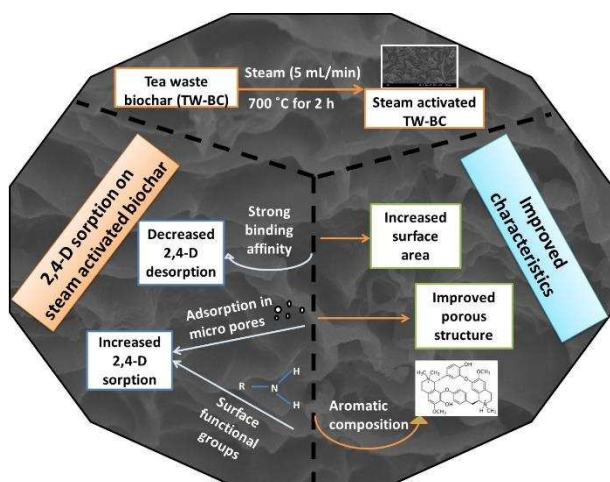
24

25 **Highlights**

- 26 1. Steam activated tea waste biochar sorbed the highest amount of 2,4-D
- 27 2. Steam activation increased biochar surface area and conserved oxygen-containing
- 28 functional groups
- 29 3. 2,4-D desorption was lowest in steam activated biochar

30

31 **Graphical abstract**



32

## 33 **Abstract**

34 Objective of this study was to investigate the mechanisms of 2,4-dichlorophenoxy acetic acid  
35 (2,4-D) sorption on biochar in aqueous solutions. Sorption isotherm, kinetics, and desorption  
36 experiments were performed to identify the role of biochars' feedstock and production  
37 conditions on 2,4-D sorption. Biochars were prepared from various green wastes (tea,  
38 burcucumber, and hardwood) at two pyrolytic temperatures (400 and 700°C). The tea waste  
39 biochar produced at 700 °C was further activated with steam under a controlled flow. The  
40 sorption of 2,4-D was strongly dependent on the biochar properties such as specific surface  
41 area, surface functional groups, and microporosity. The steam activated biochar produced  
42 from tea waste showed the highest (58.8 mg g<sup>-1</sup>) 2,4-D sorption capacity, which was  
43 attributed to the high specific surface area (576 m<sup>2</sup>g<sup>-1</sup>). The mechanism of 2,4-D removal  
44 from aqueous solution by biochar is mainly attributed to the formation of heterogeneous  
45 sorption sites due to the steam activation.

46

47 **Keywords:** 2,4-D, biochar, Pyrolysis, Physical activation, Sorption kinetics

48

## 49 1. **Introduction**

50 Agriculture activities, forestry, and maintenance of green spaces rely heavily on the use of  
51 herbicide to control weeds. The leaching and runoff from agricultural and forest land,  
52 deposition from the aerial application, and discharge of industrial wastewater to ground and  
53 surface water bodies have caused severe contamination of the environment by herbicides.  
54 Many herbicides are not easily biodegradable, and some are carcinogenic in nature, and as  
55 such represent a concerning source of environmental toxicant (Gupta et al., 2006).  
56 2,4-dichlorophenoxy acetic acid (2,4-D) is one of the oldest and more widely used herbicides  
57 (Kearns et al., 2014). 2,4-D is a systemic herbicide widely employed to selectively control  
58 broadleaf weeds. According to world health organization (WHO), 2,4-D is categorized as a

59 substance of “possibly carcinogenic to humans” (Loomis et al., 2015). It is highly soluble in  
60 water (solubility 900 mg L<sup>-1</sup>) in comparison to other organic micro-pollutants (e.g.  
61 pharmaceuticals and hydrocarbons). The pKa value of the herbicide is 2.7. Due to these  
62 reasons, removing 2,4-D from polluted waters can be challenging. The herbicide is anionic in  
63 nature, which also makes it weakly retained by intrinsically negatively charged soil and  
64 subsurface particles (Hermosin et al., 2006). This enables 2,4-D to quickly reach to the  
65 groundwater which, in many countries, is a common source of drinking water.

66 The development of an efficient, easily accessible and inexpensive technology is required for  
67 the removal of 2,4-D and other anionic herbicide compounds from water. The application of  
68 locally generated and low-cost adsorbents in water treatment processes can be a possible  
69 solution to address this issue, especially for developing countries.

70 Carbon (C) based biomass such as biochar has been used extensively to reduce toxicity levels  
71 of different pollutants in the environment (Ahmad et al., 2014; Uchimiya et al., 2010).

72 Biochar is a by-product of the thermal decomposition of various organic biomasses to  
73 produce bio-oil. This process occurs over a range of temperatures (200-800 °C) under  
74 nitrogen environment with a limited supply of oxygen (Lehmann & Joseph, 2009). In the  
75 recent years, biochar has created a broad research interests due to its surface properties, high  
76 surface area, pore volume, and pore diameter that make it a strong candidate for the removal  
77 of contaminants from soil and water bodies (Mandal et al., 2016). Furthermore, biochar has a  
78 range of oxygen-containing surface functional groups (e.g., carboxyl, phenolic, hydroxyls)  
79 which make this C-based material effective to interact with diverse types of environmental  
80 contaminants (Lehmann & Joseph, 2015).

81 However, biochar properties (surface area, pore size distribution, surface charge and  
82 functional groups) greatly depend on different parameters such as biomass sources, pyrolysis  
83 temperature, pyrolysis procedure and post-treatment processes of the product (Lehmann,  
84 2007b; Lehmann et al., 2011). From an environmental protection perspective, enhanced

85 contaminant retention capacity, faster removal/sorption kinetics and low reversibility of the  
86 sorption process are the most desirable characteristics of biochar materials.

87 Previous studies investigated the prevention of herbicide mobility in the environment through  
88 biochar application. For example, Kearns et al. (2014) found that biochar prepared from  
89 woodchips (350-700 °C), bamboo (500-700 °C) and corncobs (600 °C) adsorbed a higher  
90 quantity of 2,4-D compared to a commercial activated carbon. Similarly, Lü et al. (2012)  
91 reported that biochar produced from rice straw at 350 °C reduced the mobile 2,4-D  
92 concentration (100-600  $\mu\text{mol L}^{-1}$ ) in soils by up to 45%. In their study Lü et al. (2012) also  
93 investigated the effect of different pyrolysis temperatures (200, 350 and 500 °C) on biochar  
94 pore properties, surface functional groups and the herbicide sorption capacity.

95 The current study hypothesized that the presence of a greater surface area due to the presence  
96 of microporous structure and aromaticity or functional groups like carbonyl C=O, hydroxyl  
97 O-H and carboxyl in biochar would increase its ability to adsorb 2,4-D from aqueous  
98 solutions. In addition to the study of Lü et al. (2012) reported above there are a few other  
99 studies available on the sorption of 2,4-D by biochar (Gupta et al., 2006; Kearns et al., 2014),  
100 but none of these reports has specifically focused on a systematic investigation of the effect  
101 of feedstock source and steam activation on biochar's characteristics and their role on 2,4-D  
102 sorption. Steam activation is included in this study as it has been reported that this process  
103 can increase the degree of microporosity in biochar (Downie et al., 2009). This study  
104 underpins the feasibility of using biochar for remediating of 2,4-D and other problematic  
105 pesticides.

106

## 107 **2. Materials and methods**

### 108 **2.1. Reagents**

109 2,4-D (Sigma-Aldrich, Australia) was dissolved in ultrapure water to prepare a 1000 mg L<sup>-1</sup>  
110 stock solution. The pH of the stock solution was raised to 11 by dropwise addition of 1 N

111 sodium hydroxide (NaOH) to enhance the compound's solubility (Kearns et al., 2014). The  
112 stock solution was then stored in a dark container in a cold room (4 °C) for further use. The  
113 stock solution was diluted in 20 mM phosphate buffer saline (PBS) at pH 7 to get the targeted  
114 initial 2,4-D concentration of 100 mg L<sup>-1</sup> for the kinetic sorption experiments. Similarly, six  
115 working solutions of 2,4-D (10, 50, 100, 200, 400, and 500 mg L<sup>-1</sup>) were also prepared in  
116 PBS for conducting the sorption isotherm experiments.

117

## 118 **2.2. Biochar preparation**

119 Four different types of feedstock were used to prepare biochar in this study. They were tea  
120 waste, burcucumber, oak wood and bamboo. Tea waste was collected from a tea factory after  
121 tea leaf processing and washed several times in distilled to remove impurities. After washing  
122 the material was air-dried, crushed and ground to <1 mm in particle size for biochar  
123 preparation. Tea wastes were pyrolyzed at 700 °C with a heating rate of 7 °C min<sup>-1</sup> for 2 h  
124 using a modified N11/H Nabertherm (Germany) furnace (Ahmad et al., 2012; Rajapaksha et  
125 al., 2014). Nitrogen flow rate was set to 5 mL min<sup>-1</sup> throughout the pyrolyzation. For steam  
126 activation, samples were treated with 5 mL min<sup>-1</sup> of steam during the last 45 min of the 2 h  
127 total holding time at the peak temperature (700 °C). After steam activation, samples were  
128 allowed to cool inside the chamber to 30 °C and then the final weight was recorded. The  
129 samples from tea waste with and without steam activation were termed as TW-BC and TW-  
130 BCS, respectively.

131 Burcucumber (*Cucumis anguria*) plants were collected and dried in air, then in an oven at 60  
132 °C for 24 h. After drying, samples were ground and passed through <1 mm sieve. Crushed  
133 samples were pyrolyzed at 700 °C by following the same pyrolysis procedure used for tea  
134 waste. This biochar was termed as burcucumber biochar (BU-BC).

135 Oakwood and bamboo feedstock were collected and pyrolyzed at 400 °C for 2 h using a  
136 muffle furnace. Heating rate and N<sub>2</sub> supply were as above. After pyrolyzation, produced  
137 biochars were termed as OW-BC and B-BC.

138

### 139 **2.3. Surface characterization of biochar**

140 The pH of the biochar samples was measured using a pH meter (smartCHEM-LAB  
141 Laboratory Analyzer) in deionized water (1:10 ratio, W/V) after agitation in the end over end  
142 shaker at 20 rpm for 2 h followed by 5 min of settling time. The electrical conductivity (EC)  
143 of biochars was also measured in the same suspension using an EC electrode (smartCHEM-  
144 LAB Laboratory Analyzer) following 12 h of sediment settling. The C and N contents of  
145 biochar samples were determined with a Leco TruMac CNS Analyzer (LECO Corporation,  
146 USA). Cation exchange capacity (CEC) of the biochar samples was measured using the  
147 method described by Zelazny et al. (1996).

148 Biochar surface functional groups were determined using a Fourier-transform infrared  
149 spectrometer (FT-IR; Frontier, PerkinElmer, UK) at the wavenumber range of 600 - 4000 cm<sup>-1</sup>  
150 by potassium bromide (KBr) pellet method. Each pellet was scanned 32 times at the  
151 resolution of 0.4 cm<sup>-1</sup>. Baseline corrected spectra were used to identify the representative  
152 peaks of functional groups based on published literature (software; Thermo Nicolet). X-ray  
153 photoelectron spectroscopy (XPS) analysis was performed using a XPS spectrometer (K-  
154 Alpha, Thermo Scientific, UK) with a monochromatic Al α-Alpha radiation source, and a  
155 spot size around 400 μm in diameter with a detection limit around 0.5-1.0%. Gaussian-  
156 Lorentzian sum function was used for the XPS spectra deconvolution by XPSPEAK41.  
157 Biochar particles were also examined by field emission scanning electron microscope (FE-  
158 SEM; Hitachi S-4300, Japan) to identify the surface morphology. The specific surface area  
159 and pore volume were analyzed by the Brunauer–Emmett–Teller (BET) method at -196 °C  
160 using a Gemini 2380 Surface Area Analyzer. Pore diameter was further determined using a



161 gas sorption analyzer (NOVA-1200; Quantachrome Corp., Boynton Beach, FL, USA)  
162 (Ahmad et al., 2014).

163

#### 164 **2.4. 2,4-D sorption kinetics and isotherm**

165 2,4-D sorption experiments were performed using a batch equilibrium method. The kinetic  
166 experiment was conducted in 250 mL Schott bottle by mixing 0.25 g of each biochar sample  
167 with 100 mL of 100 mg L<sup>-1</sup> 2,4-D solution (in PBS). All the containers were wrapped with  
168 aluminum foil to maintain in darkness. The mixture was then agitated using an end-over-end  
169 shaker at room temperature (23 ± 1 °C) at 10 rpm for 72 h. Subsamples (2 mL) were taken  
170 from each bottle at different time intervals (0.25, 0.5, 1, 2, 3, 5, 7, 10, 16, 24, 36, 48, 60, and  
171 72 h). Samples were filtered using 0.45 µm cellulose ester filters immediately after  
172 collection. The filtrates after appropriate dilution were analyzed to determine 2,4-D  
173 concentrations by a spectrophotometric method at 282 nm (Aksu & Kabasakal, 2004) on a  
174 UV-VIS-NIR-Spectrophotometer (UV-3600, Shimadzu, Japan).

175 Sorption isotherms were determined at a constant pH 7 maintained by using PBS. It was  
176 found that the PBS was sufficient to control pH within ±0.2 units after addition of biochar  
177 materials (Kearns et al., 2014). Six working solutions (10, 50, 100, 200, 400, and 500 mg L<sup>-1</sup>)  
178 of 2,4-D were prepared as described above. Fifty mL centrifuge tubes were used for the  
179 isotherm experiment. The weights of tubes and lids were recorded before adding biochar and  
180 2,4-D solutions, which was needed to calculate the entrapped liquid weight and associated  
181 2,4-D concentration during desorption experiments as explained later. Exactly 0.05 g of each  
182 biochar sample was placed inside the centrifuge tube, and 20 mL of each of the 2,4-D  
183 working solutions was added to it. The samples were agitated at 10 rpm using an end-over-  
184 end shaker for 72 h at room temperature (23±1 °C). The equilibration time was decided from  
185 the sorption kinetic experiments. After equilibration samples were centrifuged at 2403-G for  
186 15 min to get clear supernatants which were further filtered using 0.45 µm cellulose ester

187 filters. The concentration of 2,4-D in the aliquot was determined by a UV-VIS-NIR-  
188 Spectrophotometer as explained earlier.

189 After removing the supernatant, the weight of tubes containing wet biochar sediments was  
190 recorded (for calculating the entrapped liquid weight). All the sorption experiments were  
191 conducted in duplicates. The labware used in this study did not sorb any 2,4-D.

192 To evaluate and compare the 2,4-D sorption capacity of different biochars, the experimental  
193 data were fitted using both Freundlich and Langmuir sorption models. The respective  
194 mathematical expressions of these models are provided as Supplementary Information (SI).  
195 Similarly, the sorption kinetic data were fitted to various kinetic models such as parabolic  
196 diffusion, elovich equation, pseudo-first order and pseudo-second order models. The  
197 mathematical expressions of these models are also given in SI.

198

## 199 **2.5. 2,4-D desorption**

200 The desorption of 2,4-D was determined following sorption of a known volume and  
201 concentration of the 2,4-D solution. Just after the sorption experiment, 20 mL deionized  
202 water was added to the sediment in each tube. Samples were agitated at 10 rpm on an end-  
203 over-end shaker for 24 h at room temperature ( $23\pm 1$  °C). The suspension was then  
204 centrifuged at 2403-G for 15 min. Clear supernatants were further filtered using 0.45  $\mu\text{m}$   
205 cellulose ester filter for 2,4-D analysis as stated above. The amount of 2,4-D which was  
206 entrapped in the wet biochar sediment coming straight from the sorption experiment was  
207 taken into consideration for calculating the respective desorption amount.

208

## 209 **2.6. Statistical analysis**

210 An analysis of variance (ANOVA) using SPSS software packages (IBM SPSS Statistics 23)  
211 was performed on the data to analyze the 2,4-D sorption capacity of different biochar  
212 samples. A post hoc t-test at 5% level of significance was also conducted to quantify the

213 significance difference between biochar samples. Variability of the data was expressed as the  
214 standard deviation (STDEV) and a p value of <0.05 was considered as statistically  
215 significant.

216

### 217 **3. Results and discussion**

#### 218 **3.1. Characterization of biochar samples**

219 The key physicochemical characteristics of biochar samples are shown in Table 1. Biochar  
220 prepared from tea waste with steam activation (TW-BCS) had a higher pH (11.9) and CEC  
221 ( $15.9 \text{ cmol}_c \text{ kg}^{-1}$ ) values compared to the other four biochars. Furthermore, BU-BC showed a  
222 higher EC value ( $1403 \mu\text{S m}^{-1}$ ) than other biochars (Table 1).

223 [Table 1]

224 The BU-BC had a much lower surface area ( $2.3 \text{ m}^2 \text{ g}^{-1}$ ; pore volume:  $0.008 \text{ cm}^3 \text{ g}^{-1}$ ) than all  
225 the other materials probably due to the lower volatile organic matter content in the  
226 burcucumber biomass than the other biomass. For example, the C content of BU-BC was  
227 very low compared to TW-BCS produced at the same temperature (Table 1). The BU-BC  
228 contains a high amount of mineral ash which does not produce a high surface area as organic  
229 material (Lehmann, 2007a). Even though feedstock characteristics is important, pyrolysis  
230 temperature also seems to have a prominent effect on the surface area of the products. For  
231 example, TW-BCS had an extremely high surface area and pore volume ( $576 \text{ m}^2 \text{ g}^{-1}$ ;  $109$   
232  $\text{cm}^3 \text{ kg}^{-1}$ ) compared to TW-BC and biochars from other two sources. Ahmad et al. (2012)  
233 reported that biochar produced at  $700 \text{ }^\circ\text{C}$  had much higher surface area than that produced at  
234 a lower temperature  $300 \text{ }^\circ\text{C}$ , which reflects the temperature effect on opening up of pore  
235 spaces due to the removal of volatile organic matters. Another study by Kloss et al. (2012)  
236 also found that increasing temperature from  $400$  to  $525 \text{ }^\circ\text{C}$  increased the surface area of wheat  
237 straw-derived biochar from  $4.8$  to  $14.2 \text{ m}^2 \text{ g}^{-1}$ .

238 Biochar usually contains a microporous structure with higher pore volume and defined pore  
239 diameter. It was observed in this study that the pore volume of steam activated tea-waste  
240 biochar was the highest ( $109 \text{ cm}^3 \text{ kg}^{-1}$ ) compared to the non-activated biochar and products  
241 produced from other biomass sources. Azargohar and Dalai (2008) also found that the  
242 physical (steam) activation increased the total pore volume of biochar samples. Similarly, an  
243 increase in the pore diameter of the biochar samples was observed as a result of steam  
244 activation (Table 1). Steam activated biochar with a large number of micropores (0-2 nm),  
245 and pore volume as shown in Table 1 could thus provide an increased herbicide sorption  
246 capacity as compared to the non-activated product (Rajapaksha et al., 2016; Rajapaksha et al.,  
247 2014). The polar surface area of 2,4-D is  $47 \text{ \AA}^2$ . The relationship between pore size/diameter  
248 and 2,4-D sorption was investigated in the previous study by Kearns et al. (2014). The  
249 authors reported that pyrolysis conditions that produced BET surface areas up to  $400 \text{ m}^2 \text{ g}^{-1}$   
250 primarily generated micropores accessible to  $\text{N}_2$ , but not 2,4-D due to the size exclusion.  
251 However, pyrolysis conditions that produced surface areas between 400 to  $600 \text{ m}^2 \text{ g}^{-1}$   
252 increased 2,4-D sorption with increasing surface area, indicating the progressive widening of  
253 micropores into the larger sized pores that accommodated 2,4-D molecules. In our study, we  
254 also found the increased surface area and pore diameter with steam activation of tea waste  
255 biochar. Moreover, these properties increased 2,4-D sorption by steam-activated biochar.  
256 Biochars produced at the higher temperature were highly carbonized and exhibited highly  
257 aromatic structures, which was shown by the FTIR data. The IR spectra showed the presence  
258 of C-H, C=O, carboxyl, phenolic and other oxygen-containing functional groups on biochar  
259 surfaces (Supplementary information).

260 The bands observed at  $3446 \text{ cm}^{-1}$  (TW-BC and TW-BCS) can be assigned to the hydroxyl (-  
261 OH) stretching vibration (Yaman, 2004). The hydroxyl groups might be decreased with steam  
262 activation due to the ignition loss of OH during the activation at high temperature (Yuan et  
263 al., 2011). Bands at  $1567$  and  $1557 \text{ cm}^{-1}$  represented the presence of strong nitro (N-O)

264 stretching vibration (Nakanishi, 1962). The presence of C=C and carbonyl (-COH) was  
265 observed at 1432 and 1431  $\text{cm}^{-1}$ , and the intensity of these groups was increased after steam  
266 activation of the biochar (Hsu et al., 2009). The increased band intensity at 1384  $\text{cm}^{-1}$   
267 represented the presence of -COOH bending vibration in the steam activated biochar  
268 (Supplementary information). Bands at 874 and 875  $\text{cm}^{-1}$  can be assigned to the aromatic C-  
269 H bending (Uchimiya et al., 2013) (Supplementary information). However, FTIR spectra did  
270 not show very significant differences between TW-BC and TW-BCS except demonstrating  
271 changes in the intensity of certain bands.

272 While FTIR data represented the bulk surface characteristics of biochar materials, XPS  
273 analysis aimed to identify the presence of specific functional groups, especially the O-  
274 containing functional groups. The O1s and C1s spectra of TW-BC and TW-BCS are  
275 presented in Fig. 1. The relative percentage of specific functional groups from O1s and C1s  
276 spectra are shown in the supplementary section. The XPS spectra showed that the O content  
277 of the steam-activated biochar (TW-BCS; O atom % = 21.04) was higher than the non-  
278 activated biochar (TW-BC; O atom % = 17.47). The peaks at binding energies of 531.3 and  
279 531.9 eV were assigned to O=C and O-C functional groups. The relative intensity of O=C  
280 and O-C functional groups are significantly higher in TW-BCS (15.6 and 73.7%) compared  
281 to TW-BC (14.4 and 59.2%) (Fig. 1a and 1b). Moreover, the relative intensity of -COOH  
282 functional groups at a binding energy of 289.3 eV is only observed in TW-BCS (Fig. 1c and  
283 1d; Supplementary information) (Liu et al., 2010). The XPS results confirmed that the steam  
284 activation could conserve a greater proportion of O-containing functional groups (e.g., -  
285 COOH as also indicated by FTIR spectra) when compared with the non-activated biochar  
286 prepared from the same feedstock.

287 [Figure 1]

288 The difference between CEC values also described the presence of effective functional  
289 groups on biochar surfaces. Previous studies found that increasing pyrolysis temperature

290 decreased the CEC value due to the loss of carboxyl functional groups during the pyrolysis  
291 process (Gai et al., 2014). However, the current study demonstrated that the steam activated  
292 biochar had the highest CEC value in comparison to other products (Table 1). Therefore,  
293 biochars produced at a similar temperature but with steam activation might help to conserve  
294 the oxygen-containing functional groups (like carboxyl), which would lead to a higher CEC  
295 value. Harvey et al. (2011) also reported that the higher CEC value of biochar might reflect  
296 the presence of a higher carboxylic group contents.

297 Scanning Electron Microscopic (SEM) images showed the morphological and structural  
298 changes between TW-BC and TW-BCS (Supplementary information). High-resolution SEM  
299 images (2000x) depicted more defined pore structure in TW-BCS compared to TW-BC. The  
300 well-defined pore structure might have caused the greater surface area in the steam activated  
301 biochar than the non-activated product (Azargohar & Dalai, 2008) (Table 1).

302

### 303 **3.2. Sorption of 2,4-D by biochar**

#### 304 3.2.1. . 2,4-D sorption kinetics

305 Several kinetic models such as parabolic diffusion, elovich equation, pseudo-first order and  
306 pseudo-second order models were tested in this study. The best kinetic model fitting was  
307 determined by considering the estimated correlation coefficient ( $R^2$ ) values, which was  
308 highest for the pseudo-second order model (Table 2). Yao et al. (2011) found that the pseudo-  
309 first order and second order models better described the phosphate removal data on biochar  
310 compared to the elovich equation. All the other model parameters presented in the  
311 supplementary information.

312 The sorption kinetic modeling allowed to calculate the sorption rate as well as explained the  
313 possible reaction mechanisms by identifying suitable rate expression characteristics. The  
314 sorption rate of 2,4-D was initially fast and then followed a slower sorption rate until  
315 gradually approaching an equilibrium (Fig. 2). The initial faster sorption might attribute to a

316 large amount of pore spaces available for the sorption (Rajapaksha et al., 2016). The steam  
317 activated biochar adsorbed 2,4-D more efficiently compared to the other products (Fig. 2).  
318 The reason could be that the steam activation enhanced the pore volume and pore diameter  
319 (Table 1) of biochar samples, which influenced the sorption process. Previous studies also  
320 found similar results, for example, Lima et al. (2010) reported that steam activation could  
321 increase the sorption ability of biochar by enhancing the pore diameter. Rajapaksha et al.  
322 (2016) found that steam activation of biochar could increase the pore size from 1.75 to 1.99  
323 nm, which consequently increased sulfamethazine sorption by the product.  
324 [Figure 2]

325 The estimated kinetic parameters for the pseudo-second order model are shown in Table 2  
326 and the parameters for the other models in supplementary information. The pseudo-first order  
327 model could be more relevant when the initial adsorbate concentration was higher, and the  
328 pseudo-second order model could be more applicable when the initial adsorbate  
329 concentration was lower (Liu, 2008). The best-fitted pseudo-second order model in the  
330 current study suggested that the sorption of 2,4-D on biochar was a function of the  
331 availability of surface sorption sites (Zhang et al., 2012). Furthermore, the best fitness of  
332 pseudo-second order model for 2,4-D sorption on biochar confirms that the sorption process  
333 may be controlled by both the physical and chemical processes (Sarkar et al., 2010). The  
334 pseudo-second order rate constant was increased from 0.04 in TW-BC to 0.21 in TW-BCS  
335 (Table 2). The K (sorption constant) value for TW-BCS was higher than for the rest of the  
336 four biochars (Table 2). This indicated that the sorption of 2,4-D on steam activated biochar  
337 was faster than the non-activated product and biochar from other sources. The kinetic  
338 sorption results of 2,4-D on biochar indicated that the feedstock composition and steam  
339 activation played a key role in the sorption process. The kinetics of sorption of the biochars  
340 followed the similar order of 2,4-D sorption capacities obtained from the sorption isotherm  
341 calculations (section 3.2.2). The difference in sorption ability could greatly depend on the

342 biochar characteristics which are a function of biomass source and production technology  
343 (Martin et al., 2012). In this study, biochar prepared at the same temperature but with steam  
344 activation enhanced the specific characteristics (surface area, pore diameter, functional  
345 groups, pH) of biochar, which led to an increased 2,4-D sorption capacity.

346 [Table 2]

347

### 348 3.2.2. 2,4-D sorption isotherm

349 Two isothermal models such as Freundlich and Langmuir were tested to fit the sorption data.  
350 The Freundlich model best described the data with  $R^2$  values of up to 0.98 (Table 3). Zhang  
351 et al. (2011) found that the sorption of simazine on biochar was best fitted to the Freundlich  
352 isotherm model with high  $R^2$  ( $>0.98$ ) values. The lower  $n$  value from the Freundlich model  
353 indicated the heterogeneous sorption domain in the sorbent and the presence of higher  
354 sorption site energy distribution (Pignatello & Xing, 1995). The fitting parameters for all  
355 attempted models are shown in the supplementary information.

356 [Figure 3]

357 Fig. 3 represents the Freundlich isotherms for the sorption of 2,4-D to five biochar samples.  
358 The steam activated biochar had the highest sorption capacity ( $58.8 \text{ mg g}^{-1}$ ) with moderate  $n$   
359 and high  $K$  and  $R^2$  values, compared to the other four biochars. The best 2,4-D sorption  
360 fitness with Freundlich model compared to Langmuir model suggests the formation of more  
361 heterogeneous sorption sites on biochar because of the steam activation (Rusmin et al., 2015).  
362 In general, 2,4-D sorption capacity decreased in the order: TW-BCS>OW-BC>BU-BC>B-  
363 BC>TW-BC. For TW-BC and TW-BCS, some nonlinearity was observed at low adsorbate  
364 concentration, but the linearity increased with increasing 2,4-D concentrations. The high  
365 sorption on TW-BCS might be attributed to the high surface area of the biochar. Previous  
366 studies also supported our findings, for example, Ahmad et al. (2012) observed that biochar  
367 prepared at a higher temperature with high surface area ( $448.2 \text{ m}^2 \text{ g}^{-1}$ ) removed



368 trichloroethylene (TCE) more efficiently than that prepared at a lower temperature (300 °C;  
369 surface area: 3.14 m<sup>2</sup> g<sup>-1</sup>). Few authors also found that biochar with a lower surface area  
370 could adsorb more 2,4-D than biochar with a higher surface area. For example, Lü et al.  
371 (2012) found that biochar produced from rice straw at 300 °C (20.6 m<sup>2</sup>g<sup>-1</sup>) could adsorb 2,4-D  
372 more than biochar at 500 °C (128 m<sup>2</sup>g<sup>-1</sup>). The reason could be the difference in the chemical  
373 composition between the biochar samples which played an important role in increasing the  
374 sorption capacity at low temperature despite having a lower surface area (Lü et al., 2012).  
375 In order to better compare the sorption ability of biochar to those of other sorbents, the  
376 sorption distribution coefficient ( $K_d$ ) was calculated (Table 4). The  $K_d$  values were  
377 normalized to organic carbon content ( $K_{oc}$ ). The formula for  $K_d$  and  $K_{oc}$  is presented in the  
378 supplementary information. Within the tested concentration ranges, the  $K_d$  value was on the  
379 order of 10<sup>3</sup> (L kg<sup>-1</sup>) for TW-BCS. The observed  $K_d$  values are much larger than those  
380 reported in the previous studies for natural geo-sorbents, including soils ( $K_d < 10$  L kg<sup>-1</sup>),  
381 humic substances, and clay minerals ( $K_d < 100$  L kg<sup>-1</sup>) (Ji et al., 2009) and less than those  
382 recorded for black carbon ( $K_d < 10^6$  L kg<sup>-1</sup>) (Teixidó et al., 2011). The  $K_d$  values of 2,4-D by  
383 TW-BCS was significantly higher than biochar produced from other sources. Also, the  
384 sorption studies showed a higher 2,4-D removal by TW-BCS than other biochar samples. The  
385 reason could be attributed to the microporous nature, higher surface area and aromatic carbon  
386 structure of the TW-BCS materials. Our findings are supported by previous research, such as  
387 Ren et al. (2016) found that the sorption affinity of phenanthrene to biochar (700 °C) was  
388 significantly higher than biochar (300 °C) because of microporous nature and higher surface  
389 area of biochar (700 °C). Moreover, from Table 4 the increased  $K_{oc}$  value for TW-BCS was  
390 also observed.  $K_{oc}$  values are useful to estimate the relative affinity and attraction of the  
391 herbicide to the biochar materials. Therefore, it also predicts the herbicide mobility in the  
392 solution (Futch & Singh, 1999). Higher  $K_{oc}$  values correlate with the greater sorption of 2,4-  
393 D by biochar samples whereas lower  $K_{oc}$  values represent the higher mobility of 2,4-D in

394 solution (Buttler et al., 1991). Therefore, sorption of 2,4-D to steam activated biochar was  
395 much higher compared to non-activated biochar due to having improved surface properties.

396 [Table 3]

397 [Table 4]

### 398 3.2.3. 2,4-D desorption

399 The sorbed 2,4-D by a single extraction with deionized water only removed 4.4 to 21.5% of  
400 2,4-D that was sorbed. A maximum 21.5% of 2,4-D desorption was observed in the case of  
401 TW-BC, whereas the lowest desorption was observed in the case of TW-BCS (4.4%). This  
402 indicated that the steam activated biochar had a stronger binding affinity to 2,4-D compare to  
403 other biochars. This also implied that biochar with steam activation held a lesser risk of  
404 possible release of adsorbed 2,4-D into the environment. The reason could be the diffusion  
405 process that might limit/decrease the desorption of 2,4-D from steam activated biochar (TW-  
406 BCS) (Ahmad et al., 2012). Loganathan et al. (2009) observed that the herbicide atrazine  
407 remained much higher (five times) in the char-amended soil after desorption and washing  
408 steps compared to soil alone. Desorption of pesticides like carbofuran from biochar prepared  
409 from red gum wood (*Eucalyptus* spp.) was also less than the control due to the strong  
410 sorption of pesticide on biochar surface (Yu et al., 2009).

411

## 412 **4. Conclusions**

413 Results of this research demonstrated that the laboratory prepared biochars could adsorb 2,4-  
414 D from solution. Sorption studies showed that the steam activated biochar adsorbed 2,4-D  
415 more efficiently than its non-steam activated biochars. Due to having a higher surface area,  
416 pore volume, and pore diameter the steam activated biochar showed a higher 2,4-D sorption  
417 capacity. Furthermore, a reduced 2,4-D desorption indicated that the steam activated biochar  
418 could also retain 2,4 D more efficiently. Future studies should focus more in detail on the

419 mechanism of herbicide sorption and retention of a range of activated biochars in comparison  
420 to their conventionally prepared counterparts.

421

422 E-supplementary data for this work can be found in e-version of this paper online.

423

#### 424 **Acknowledgments**

425 Sanchita Mandal is thankful to the Department of Education and Training, Government of  
426 Australia, for awarding her an Australian Postgraduate Award (APA).

427

#### 428 **Reference**

429 Ahmad, M., Lee, S.S., Dou, X., Mohan, D., Sung, J.-K., Yang, J.E., Ok, Y.S. 2012. Effects of  
430 pyrolysis temperature on soybean stover- and peanut shell-derived biochar properties  
431 and TCE adsorption in water. *Bioresource Technology*, **118**, 536-544.

432 Ahmad, M., Rajapaksha, A.U., Lim, J.E., Zhang, M., Bolan, N., Mohan, D., Vithanage, M.,  
433 Lee, S.S., Ok, Y.S. 2014. Biochar as a sorbent for contaminant management in soil  
434 and water: a review. *Chemosphere*, **99**, 19-33.

435 Aksu, Z., Kabasakal, E. 2004. Batch adsorption of 2, 4-dichlorophenoxy-acetic acid (2, 4-D)  
436 from aqueous solution by granular activated carbon. *Separation and Purification  
437 Technology*, **35**(3), 223-240.

438 Azargohar, R., Dalai, A.K. 2008. Steam and KOH activation of biochar: Experimental and  
439 modeling studies. *Microporous and Mesoporous Materials*, **110**(2-3), 413-421.

440 Buttler, T., Hornsby, A., Tucker, D., Knapp, J., Noling, J. 1991. Citrus: managing pesticides  
441 for crop production and water quality protection: a supplement to the IFAS pest  
442 control guides. Circular-Florida Cooperative Extension Service (USA).

443 Cao, X., Ma, L., Gao, B., Harris, W. 2009. Dairy-manure derived biochar effectively sorbs  
444 lead and atrazine. *Environmental Science & Technology*, **43**(9), 3285-3291.

- 445 Chakravarty, S., Dureja, V., Bhattacharyya, G., Maity, S., Bhattacharjee, S. 2002. Removal  
446 of arsenic from groundwater using low cost ferruginous manganese ore. *Water*  
447 *research*, **36**(3), 625-632.
- 448 Downie, A., Crosky, A., Munroe, P. 2009. Physical properties of biochar. *Biochar for*  
449 *environmental management: Science and technology*, 13-32.
- 450 Futch, S., Singh, M. 1999. Herbicide mobility using soil leaching columns. *Bulletin of*  
451 *environmental contamination and toxicology*, **62**(5), 520-529.
- 452 Gai, X., Wang, H., Liu, J., Zhai, L., Liu, S., Ren, T., Liu, H. 2014. Effects of feedstock and  
453 pyrolysis temperature on biochar adsorption of ammonium and nitrate. *PloS one*,  
454 **9**(12), e113888.
- 455 Gerente, C., Lee, V., Cloirec, P.L., McKay, G. 2007. Application of chitosan for the removal  
456 of metals from wastewaters by adsorption—mechanisms and models review. *Critical*  
457 *Reviews in Environmental Science and Technology*, **37**(1), 41-127.
- 458 Gupta, V.K., Ali, I., Suhas, Saini, V.K. 2006. Adsorption of 2,4-D and carbofuran pesticides  
459 using fertilizer and steel industry wastes. *Journal of Colloid and Interface Science*,  
460 **299**(2), 556-563.
- 461 Harvey, O.R., Herbert, B.E., Rhue, R.D., Kuo, L.-J. 2011. Metal interactions at the biochar-  
462 water interface: energetics and structure-sorption relationships elucidated by flow  
463 adsorption microcalorimetry. *Environmental science & technology*, **45**(13), 5550-  
464 5556.
- 465 Hermosin, M., Celis, R., Facenda, G., Carrizosa, M., Ortega-Calvo, J., Cornejo, J. 2006.  
466 Bioavailability of the herbicide 2, 4-D formulated with organoclays. *Soil biology and*  
467 *Biochemistry*, **38**(8), 2117-2124.
- 468 Hsu, N.-H., Wang, S.-L., Liao, Y.-H., Huang, S.-T., Tzou, Y.-M., Huang, Y.-M. 2009.  
469 Removal of hexavalent chromium from acidic aqueous solutions using rice straw-  
470 derived carbon. *Journal of hazardous materials*, **171**(1), 1066-1070.

471 Inyang, M., Gao, B., Ding, W., Pullammanappallil, P., Zimmerman, A.R., Cao, X. 2011.  
472 Enhanced lead sorption by biochar derived from anaerobically digested sugarcane  
473 bagasse. *Separation Science and Technology*, **46**(12), 1950-1956.

474 Ji, L., Chen, W., Zheng, S., Xu, Z., Zhu, D. 2009. Adsorption of sulfonamide antibiotics to  
475 multiwalled carbon nanotubes. *Langmuir*, **25**(19), 11608-11613.

476 Kearns, J.P., Wellborn, L.S., Summers, R.S., Knappe, D.R.U. 2014. 2,4-D adsorption to  
477 biochars: Effect of preparation conditions on equilibrium adsorption capacity and  
478 comparison with commercial activated carbon literature data. *Water Research*, **62**, 20-  
479 28.

480 Kloss, S., Zehetner, F., Dellantonio, A., Hamid, R., Ottner, F., Liedtke, V., Schwanninger,  
481 M., Gerzabek, M.H., Soja, G. 2012. Characterization of slow pyrolysis biochars:  
482 effects of feedstocks and pyrolysis temperature on biochar properties. *Journal of*  
483 *environmental quality*, **41**(4), 990-1000.

484 Lehmann, J. 2007a. Bio-energy in the black. *Frontiers in Ecology and the Environment*, **5**(7),  
485 381-387.

486 Lehmann, J. 2007b. A handful of carbon. *Nature*, **447**(7141), 143-144.

487 Lehmann, J., Joseph, S. 2009. *Biochar for environmental management: science and*  
488 *technology*. Earthscan.

489 Lehmann, J., Joseph, S. 2015. *Biochar for environmental management: science, technology*  
490 *and implementation*. Routledge.

491 Lehmann, J., Rillig, M.C., Thies, J., Masiello, C.A., Hockaday, W.C., Crowley, D. 2011.  
492 Biochar effects on soil biota - A review. *Soil Biology and Biochemistry*, **43**(9), 1812-  
493 1836.

494 Lima, I.M., Boateng, A.A., Klasson, K.T. 2010. Physicochemical and adsorptive properties  
495 of fast-pyrolysis bio-chars and their steam activated counterparts. *Journal of chemical*  
496 *technology and biotechnology*, **85**(11), 1515-1521.

497 Liu, S., Sun, J., Huang, Z. 2010. Carbon spheres/activated carbon composite materials with  
498 high Cr (VI) adsorption capacity prepared by a hydrothermal method. *Journal of*  
499 *hazardous materials*, **173**(1), 377-383.

500 Liu, Y. 2008. New insights into pseudo-second-order kinetic equation for adsorption.  
501 *Colloids and Surfaces A: Physicochemical and Engineering Aspects*, **320**(1), 275-278.

502 Loganathan, V.A., Feng, Y., Sheng, G.D., Clement, T.P. 2009. Crop-residue-derived char  
503 influences sorption, desorption and bioavailability of atrazine in soils. *Soil Science*  
504 *Society of America Journal*, **73**(3), 967-974.

505 Loomis, D., Guyton, K., Grosse, Y., El Ghissasi, F., Bouvard, V., Benbrahim-Tallaa, L.,  
506 Guha, N., Mattock, H., Straif, K., IARC, L. 2015. Carcinogenicity of lindane, DDT,  
507 and 2, 4-dichlorophenoxyacetic acid. *The Lancet. Oncology*, **16**(8), 891.

508 Lü, J., Li, J., Li, Y., Chen, B., Bao, Z. 2012. Use of rice straw biochar simultaneously as the  
509 sustained release carrier of herbicides and soil amendment for their reduced leaching.  
510 *Journal of agricultural and food chemistry*, **60**(26), 6463-6470.

511 Mandal, S., Sarkar, B., Bolan, N., Ok, Y.S., Naidu, R. 2016. Enhancement of chromate  
512 reduction in soils by surface modified biochar. *Journal of environmental*  
513 *management*.

514 Martin, S.M., Kookana, R.S., Van Zwieten, L., Krull, E. 2012. Marked changes in herbicide  
515 sorption–desorption upon ageing of biochars in soil. *Journal of Hazardous Materials*,  
516 **231–232**, 70-78.

517 Nakanishi, K. 1962. *Infrared absorption spectroscopy, practical*.

518 Pignatello, J.J., Xing, B. 1995. Mechanisms of slow sorption of organic chemicals to natural  
519 particles. *Environmental Science & Technology*, **30**(1), 1-11.

520 Rajapaksha, A.U., Vithanage, M., Lee, S.S., Seo, D.-C., Tsang, D.C.W., Ok, Y.S. 2016.  
521 Steam activation of biochars facilitates kinetics and pH-resilience of sulfamethazine  
522 sorption. *Journal of Soils and Sediments*, **16**(3), 889-895.

523 Rajapaksha, A.U., Vithanage, M., Zhang, M., Ahmad, M., Mohan, D., Chang, S.X., Ok, Y.S.  
524 2014. Pyrolysis condition affected sulfamethazine sorption by tea waste biochars.  
525 *Bioresource technology*, **166**, 303-308.

526 Ren, X., Yuan, X., Sun, H. 2016. Dynamic changes in atrazine and phenanthrene sorption  
527 behaviors during the aging of biochar in soils. *Environmental Science and Pollution*  
528 *Research*, 1-10.

529 Rusmin, R., Sarkar, B., Liu, Y., McClure, S., Naidu, R. 2015. Structural evolution of  
530 chitosan–palygorskite composites and removal of aqueous lead by composite beads.  
531 *Applied Surface Science*, **353**, 363-375.

532 Sarkar, B., Xi, Y., Megharaj, M., Krishnamurti, G.S.R., Rajarathnam, D., Naidu, R. 2010.  
533 Remediation of hexavalent chromium through adsorption by bentonite based  
534 Arquad® 2HT-75 organoclays. *Journal of Hazardous Materials*, **183**(1–3), 87-97.

535 Teixidó, M., Pignatello, J.J., Beltrán, J.L., Granados, M., Peccia, J. 2011. Speciation of the  
536 ionizable antibiotic sulfamethazine on black carbon (biochar). *Environmental science*  
537 *& technology*, **45**(23), 10020-10027.

538 Uchimiya, M., Lima, I.M., Thomas Klasson, K., Chang, S., Wartelle, L.H., Rodgers, J.E.  
539 2010. Immobilization of heavy metal ions (CuII, CdII, NiII, and PbII) by broiler litter-  
540 derived biochars in water and soil. *Journal of Agricultural and Food Chemistry*,  
541 **58**(9), 5538-5544.

542 Uchimiya, M., Orlov, A., Ramakrishnan, G., Sistani, K. 2013. In situ and ex situ  
543 spectroscopic monitoring of biochar's surface functional groups. *Journal of Analytical*  
544 *and Applied Pyrolysis*, **102**, 53-59.

545 Wang, S., Gao, B., Li, Y., Mosa, A., Zimmerman, A.R., Ma, L.Q., Harris, W.G., Migliaccio,  
546 K.W. 2015. Manganese oxide-modified biochars: Preparation, characterization, and  
547 sorption of arsenate and lead. *Bioresource Technology*, **181**, 13-17.

548 Wang, X.S., Chen, L.F., Li, F.Y., Chen, K.L., Wan, W.Y., Tang, Y.J. 2010. Removal of Cr  
549 (VI) with wheat-residue derived black carbon: reaction mechanism and adsorption  
550 performance. *Journal of hazardous materials*, **175**(1), 816-822.

551 Yaman, S. 2004. Pyrolysis of biomass to produce fuels and chemical feedstocks. *Energy*  
552 *conversion and management*, **45**(5), 651-671.

553 Yao, Y., Gao, B., Inyang, M., Zimmerman, A.R., Cao, X., Pullammanappallil, P., Yang, L.  
554 2011. Removal of phosphate from aqueous solution by biochar derived from  
555 anaerobically digested sugar beet tailings. *Journal of Hazardous Materials*, **190**(1-3),  
556 501-507.

557 Yu, X.-Y., Ying, G.-G., Kookana, R.S. 2009. Reduced plant uptake of pesticides with biochar  
558 additions to soil. *Chemosphere*, **76**(5), 665-671.

559 Yuan, J.-H., Xu, R.-K., Zhang, H. 2011. The forms of alkalis in the biochar produced from  
560 crop residues at different temperatures. *Bioresource Technology*, **102**(3), 3488-3497.

561 Zelazny, L.W., He, L., Vanwormhoudt, A. 1996. Charge analysis of soils and anion  
562 exchange. *Methods of Soil Analysis Part 3—Chemical Methods(methodsofsoilan3)*,  
563 1231-1253.

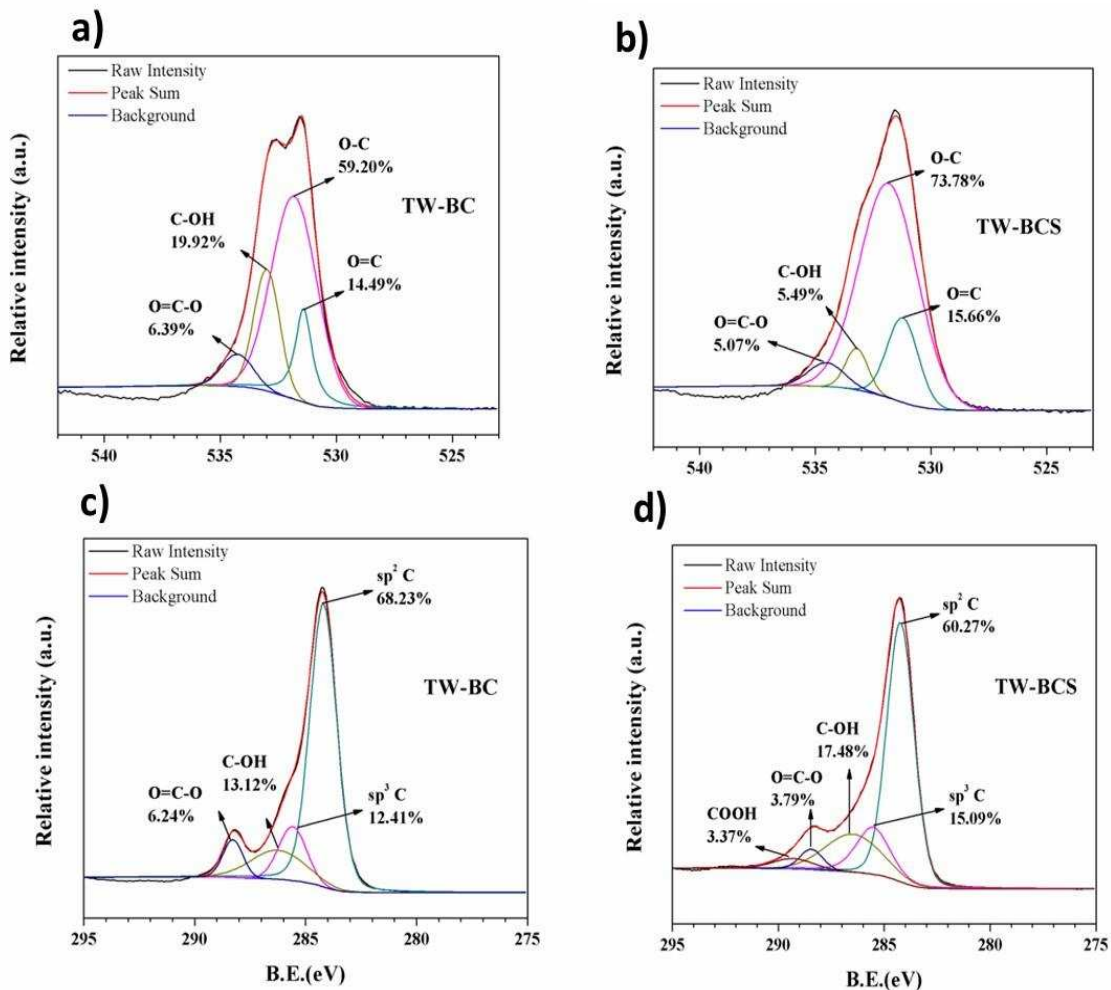
564 Zhang, G., Zhang, Q., Sun, K., Liu, X., Zheng, W., Zhao, Y. 2011. Sorption of simazine to  
565 corn straw biochars prepared at different pyrolytic temperatures. *Environmental*  
566 *Pollution*, **159**(10), 2594-2601.

567 Zhang, M., Gao, B., Yao, Y., Xue, Y., Inyang, M. 2012. Synthesis, characterization, and  
568 environmental implications of graphene-coated biochar. *Science of the Total*  
569 *Environment*, **435-436**, 567-572.

570

571





573

574

575

576 Figure 1: X-ray photoelectron spectroscopy (XPS) spectra of biochar samples: (a) O1 spectra

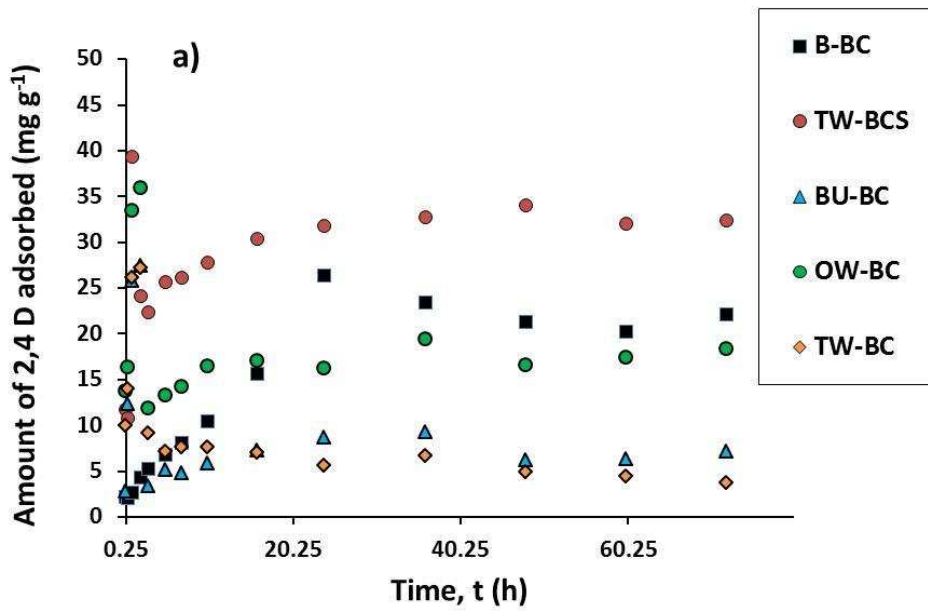
577 for TW-BC, (b) O1 spectra for TW-BCS, (c) C1s spectra for TW-BC, and (d) C1s spectra for

578 TW-BCS

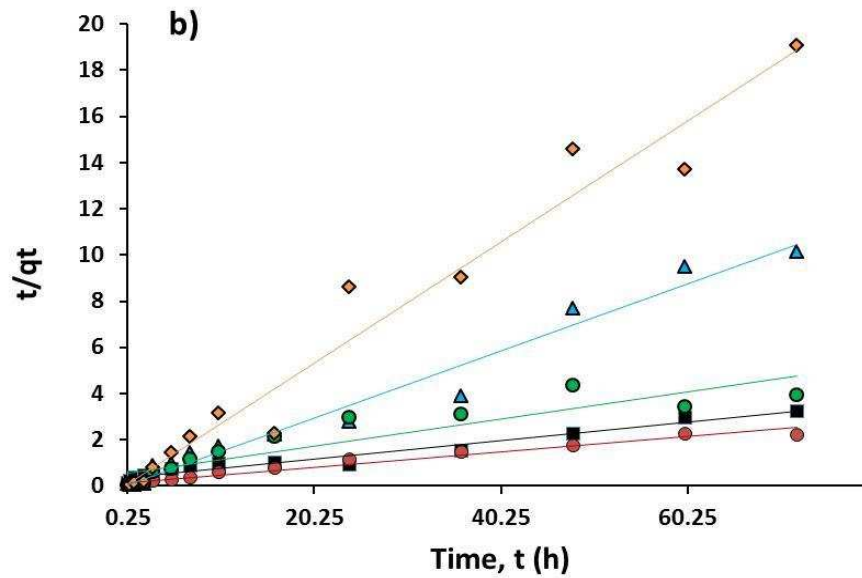
579 TW-BC: Tea waste biochar; TW-BCS: Steam activated tea waste biochar

580

581



582

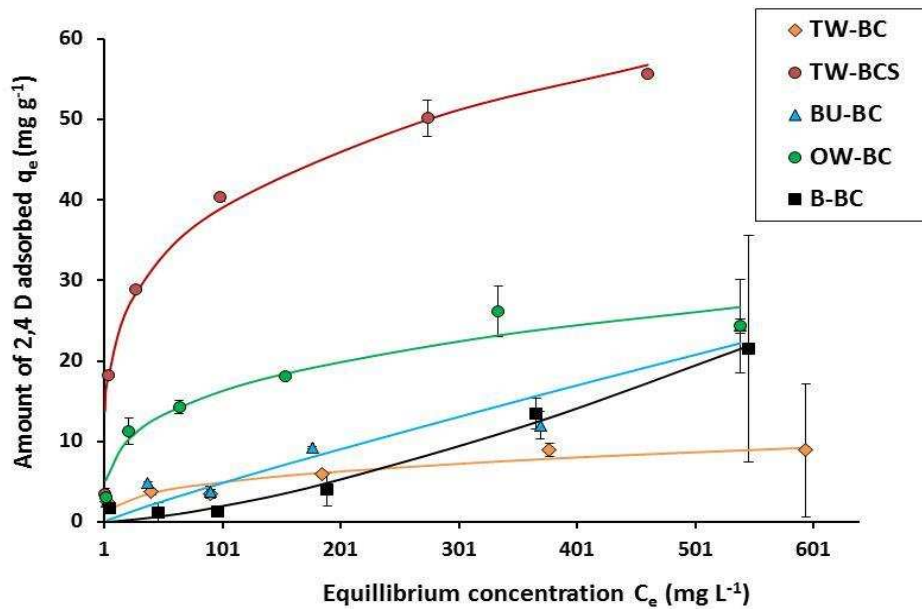


583

584 Figure 2: 2,4-D sorption kinetics on tea waste biochar (TW-BC), steam activated steam waste  
585 biochar (TW-BCS), burcucumber biochar (BU-BC), oak wood biochar (OW-BC) and  
586 bamboo biochar (B-BC) (a) sorption data; (b) amount of 2,4-D sorbed at time t (t/qt) (pseudo-  
587 second order kinetic model fitting)

588

589



590

591 Figure 3: 2,4-D sorption isotherms on tea waste biochar (TW-BC), steam activated steam  
 592 waste biochar (TW-BCS), burcucumber biochar (BU-BC), oak wood biochar (OW-BC) and  
 593 bamboo biochar (B-BC) with Freundlich model fitting. Error bars represent the standard  
 594 deviation

595

596 **Tables**

597 Table 1: Physicochemical properties of five different biochar samples. Pore diameter and pore volume data were collected from Rajapaksha et al.  
598 (2014) and Vithanage et al. (2015)

<b>Sample name</b>	<b>Pyrolysis temperature ( °C)</b>	<b>pH</b>	<b>EC (<math>\mu\text{S m}^{-1}</math>)</b>	<b>CEC (<math>\text{cmol}_c \text{ kg}^{-1}</math>)</b>	<b>C%</b>	<b>N%</b>	<b>Surface area (<math>\text{m}^2 \text{ g}^{-1}</math>)</b>	<b>Pore volume (<math>\text{cm}^3 \text{ kg}^{-1}</math>)</b>	<b>Pore diameter (nm)</b>
TW-BC	700	10.8±0.06	62.7±0.35	2.3±0.15	72.8±0.25	3.7±0.09	421.3	57.6	1.9
TW-BCS	700	11.9±0.02	221.4±0.25	15.9±1.16	63.4±0.73	3.4±0.07	576.1	109.1	2.0
BU-BC	700	10.7±0.12	1403.3±0.21	2.5±5.29	43.8±0.19	3.2±0.01	2.3	8.4	0.7
OW-BC	400	10.4±0.22	73.7±0.31	2.6±0.31	84.3±0.57	0.8±0.03	270.7	120.0	1.1
B-BC	400	10.2±0.23	24.9±0.41	3.6±0.75	86.2±0.12	0.6±0.03	475.6	209.0	1.1

599 TW-BC: Tea waste biochar; TW-BCS: Steam activated tea waste biochar; BU-BC: Burcucumber biochar; OW-BC: Oak wood biochar; B-BC:

600 Bamboo biochar; EC: Electrical conductivity; CEC: Cation exchange capacity; ± indicates the standard deviation (STD) values

601

602 Table 2: Fitted parameters values of sorption kinetic model (Pseudo-second order model)

Biochar	Pseudo-second order model parameters		
	$Q_t$ Amount of 2,4-D adsorbed at time t (mg g <sup>-1</sup> min <sup>-1</sup> )	$K_2$ (sorption constant)	$R^2$
TW-BCS	71.50	0.21	0.96
TW-BC	50.42	0.04	0.99
BU-BC	27.62	0.09	0.98
OW-BC	39.52	0.02	0.95
B-BC	2.68	0.17	0.96

603 TW-BC: Tea waste biochar, TW-BCS: Steam activated tea waste biochar, BU-BC:

604 Burcucumber biochar, OW-BC: Oak wood biochar, and B-BC: Bamboo biochar; Kinetic

605 models are presented in the supplementary information

606

607 Table 3. Freundlich and Langmuir model parameters for sorption isotherm of 2,4-D on  
 608 biochar

Biochar	Freundlich model parameter		
	K (sorption constant)	N (slope of sorption isotherm)	R <sup>2</sup>
TW-BC	3.52	0.06	0.98
TW-BCS	3.63	0.75	0.98
BU-BC	0.22	0.30	0.85
OW-BC	2.23	0.39	0.94
B-BC	0.08	0.21	0.76
Biochar	Langmuir model parameter		
	K <sub>f</sub> (sorption constant)	Q (maximum sorption capacity mg g <sup>-1</sup> )	R <sup>2</sup>
TW-BC	0.02	10.05	0.96
TW-BCS	0.01	58.85	0.97
BU-BC	0.02	42.67	0.74
OW-BC	0.02	26.66	0.90
B-BC	0.04	28.92	0.71

609 TW-BC: Tea waste biochar, TW-BCS: Steam activated TW-BC, BU-BC: Burcucumber  
 610 biochar, OW-BC: Oak wood biochar, B-BC: Bamboo biochar. Isotherm models are  
 611 expressed in the supplementary information

612

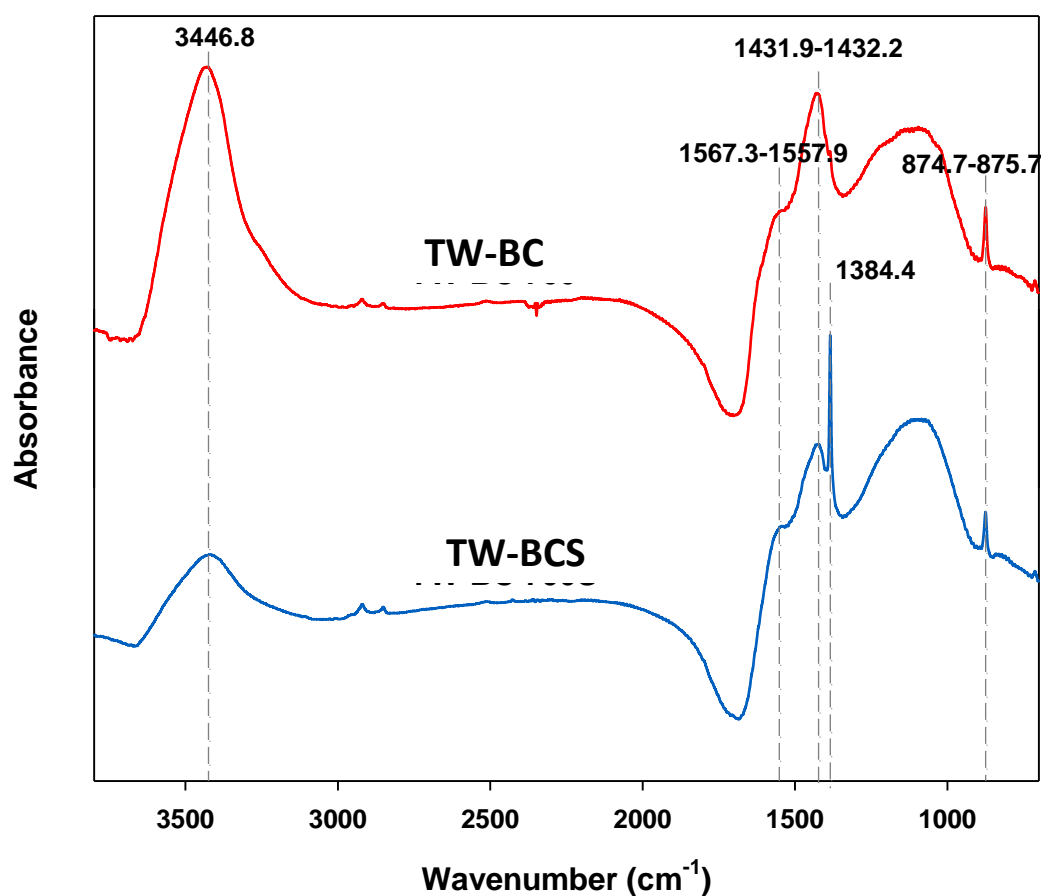
613 Table 4: Distribution sorption coefficient ( $K_d$  and  $K_{oc}$ ) of 2,4-D sorption for biochar samples

<b>Biochar sample</b>	<b><math>K_d</math> (L kg<sup>-1</sup>)</b>	<b><math>K_{oc}</math> (L kg<sup>-1</sup>)</b>
TW-BC	148.27	203.67
TW-BCS	1452.51	2291.02
BU-BC	155.72	355.53
OW-BC	404.68	480.05
B-BC	73.70	157.17

614 Tea waste biochar (TW-BC), steam activated tea waste biochar (TW-BCS), burcucumber

615 biochar (BU-BC), oak wood biochar (OW-BC), and bamboo biochar (B-BC)

616

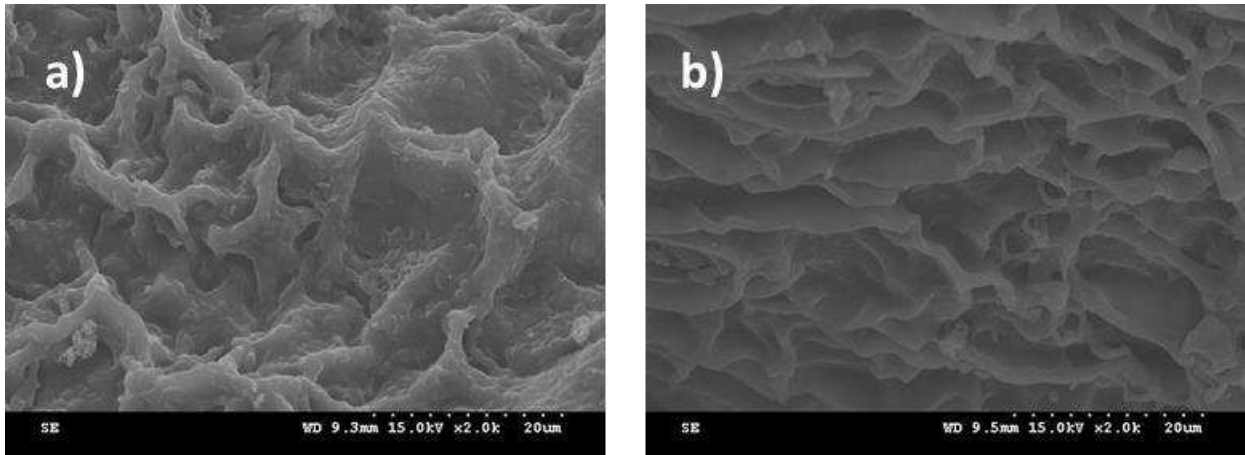


618

619 Figure 1: Fourier transform infrared spectroscopy (FTIR) spectrum to confirm the presence of  
620 functional groups on TW-BC (Tea waste biochar) and TW-BCS (steam activated tea waste  
621 biochar)

622





624

625 Figure 2: Scanning Electron Microscope (SEM) images of the surface of biochar: (a) tea  
 626 waste biochar (TW-BC), and (b) steam activated tea waste biochar (TW-BCS)

627

### 628 Sorption models:

629 2,4-D sorption kinetic models were fitted by Parabolic diffusion, Elovich, Pseudo-first order  
 630 and Pseudo-second order models. The respective equation can be expressed as follows (Wang  
 631 et al., 2015; Yao et al., 2011)

### 632 Parabolic diffusion model

$$633 \quad Q_t = A + R \times t^{1/2} \quad Eq. 1$$

### 634 Elovich model

$$635 \quad Q_t = \frac{1}{\beta} \ln(\alpha\beta) + \frac{1}{\beta} \ln(t) \quad Eq. 2$$

### 636 Pseudo-first order model

$$637 \quad \ln(Q_{e_1} - Q_t) = \ln(Q_{e_1} - K_1 t) \quad Eq. 3$$

638

### 639 Pseudo-second order model

$$640 \quad t/Q_t = 1(K_2^2 Q_{e_2}^2) + t/Q_{e_2} \quad Eq. 4$$

641 Where, Where,  $q_t$ = amount of 2,4-D adsorbed at time t ( $\text{mg g}^{-1}\text{min}^{-1}$ ), A = is the initial  
 642 sorption rate ( $\text{mg g}^{-1}\text{min}^{-1}$ ),  $\alpha$ ,  $\beta$  and R= Parabolic and Elovich model sorption constant,  $q_{e_1}$   
 643 and  $q_{e_2}$ = sorption capacity at equilibrium ( $\text{mg g}^{-1}$ ) for Pseudo first order and second order,  $K_1$   
 644 and  $K_2$  = pseudo-first and second order constant and t = is the time (min). The Pseudo-first  
 645 order and second order models describe the kinetics of the solid-solution based mononuclear  
 646 and binuclear sorption respectively while considering the sorbent capacity (Gerente et al.,  
 647 2007; Wang et al., 2010). Parabolic diffusion and Elovich models are empirical equations  
 648 considering the contribution of desorption.

649 Sorption isotherm data were tested using Freundlich and Langmuir models, and the equations  
 650 for the respective models can be written as follows (Yao et al., 2011)

651 **Langmuir model**

652 
$$Q_e = \frac{K_f Q C_e}{1 + K_f C_e} \quad \text{Eq. 5}$$

653 **Freundlich model**

654 
$$Q_e = K C_e^n \quad \text{Eq. 6}$$

655 Where,  $Q_e$  = Amount of 2,4-D adsorbed per unit weight of biochar samples ( $\text{mg g}^{-1}$ ),  $C_e$  = the  
 656 equilibrium concentration of the solution ( $\text{mg L}^{-1}$ ),  $K_f$  and  $K$  = the Langmuir and Freundlich  
 657 sorption constant,  $Q$ = Langmuir maximum sorption capacity ( $\text{mg g}^{-1}$ ),  $n$  = slope of sorption  
 658 isotherm. Langmuir model indicates the monolayer sorption into the homogeneous surface  
 659 with no interaction between the adsorbed sorbent, while the Freundlich model is an empirical  
 660 model often used to describe the chemisorption into the heterogeneous surface (Cao et al.,  
 661 2009; Chakravarty et al., 2002; Inyang et al., 2011).

662

663

664 Table 1: Fitted parameters values of sorption kinetic models (Pseudo-first order model,  
 665 Parabolic diffusion model, and Elovich model)

Biochar	Pseudo-first order model parameters		
	Q <sub>t</sub> Amount of 2,4-D adsorbed at time t (mg g <sup>-1</sup> min <sup>-1</sup> )	K <sub>1</sub> (sorption constant)	R <sup>2</sup>
TW-BCS	61.713	0.017	0.775
TW-BC	27.175	0.033	0.688
BU-BC	24.461	0.089	0.966
OW-BC	12.5698	0.018	0.664
B-BC	14.260	0.008	0.808
Biochar	Parabolic diffusion model		
	A Initial sorption rate (mg g <sup>-1</sup> min <sup>-1</sup> )	R (sorption constant)	R <sup>2</sup>
TW-BCS	7.483	3.011	0.825
TW-BC	5.855	46.025	0.694
BU-BC	2.818	4.979	0.951
OW-BC	1.477	33.807	0.523
B-BC	-2.117	26.743	0.721
Biochar	Elovich model		
	α sorption constant (mg g <sup>-1</sup> min <sup>-1</sup> )	β (sorption constant)	R <sup>2</sup>
TW-BCS	11.163	8.709	0.826
TW-BC	10.176	44.344	0.927
BU-BC	4.064	7.401	0.889

OW-BC	1.196	35.588	0.397
B-BC	-3.184	25.165	0.736

666 TW-BC: Tea waste biochar, TW-BCS: Steam activated tea waste biochar, BU-BC:  
667 Burcucumber biochar, OW-BC: Oak wood biochar, and B-BC: Bamboo biochar; Kinetic  
668 models are presented in the supplementary information

669

670 **Distribution coefficient:**

671 The sorption distribution coefficient ( $K_d$ ) was calculated by,

672 
$$K_d = \frac{Q_e}{C_e} \quad Eq. 7$$

673 Where,  $K_d$  = distribution coefficient ( $L\ kg^{-1}$ ),  $Q_e$  = amount of 2,4-D adsorbed ( $mg\ kg^{-1}$ ) and  
674  $C_e$  = equilibrium concentration of 2,4-D ( $mg\ L^{-1}$ )

675

676 Organic-carbon normalized  $K_d$  ( $K_{oc}$ ) was calculated by,

677 
$$K_{oc} = (K_d/\%C) \times 100 \quad Eq. 8$$

678 Where,  $K_{oc}$ = distribution coefficient ( $L\ kg^{-1}$ ),  $C$ = organic carbon content (%)

679

680 XPS analysis:

681 Table 2. Assignments of O1s and C1s characteristic peaks deconvoluted from XPS spectra  
682 (Liu et al., 2010) and its relative percentage in samples

Peak	Position (eV)	TW-BC	TW-BCS
O=C	531.3	22684.97	26429.98
O-C	531.9	92661.88	124493.60
C-OH	533.2	31181.91	9265.60
O=C-O	534.3	9999.22	8549.08

683	sp <sup>2</sup> C	284.2	207732.00	149724.40
684	sp <sup>3</sup> C	285.6	37783.74	37485.90
685	C-OH	286.3	39958.59	43424.45
686	O=C-O	288.3	19005.29	9404.57
687	COOH	289.3	0	8382.50
688				

689 TW-BC: Tea waste biochar; TW-BCS: Steam activated tea waste biochar

690